Supporting Material

Additional Text:

GBD-Clr4-∆cd mediated silencing is locus and marker gene independent

The GBD-Clr4, GBD-Clr4-∆cd and GBD-Clr4-∆cd-H410K fusion proteins expressed from the *clr4* promoter at the *clr4* locus are produced and detected in cells at similar levels (fig. S1A). The GBD-Clr4-∆cd protein can silence the *3xgbs-ade6*$^+$ or *10xgbs-ura4*$^+$ reporters at the *ura4* or *arg3* loci (fig. 1A; fig. S1B, C) indicating that this silencing is independent of the location of the Gal4 binding sites in the genome and the adjacent marker gene. Consistent with these observations, silencing of marker genes also occurs in the context of plasmid-based minichromosomes (see fig. S8). Anti-Gal4 binding domain ChIP indicate that the GBD-Clr4-∆cd fusion protein is recruited to the Gal4 binding sites adjacent to the *ura4::3xgbs-ade6*$^+$ reporter (fig. S1D) and on the plasmid-based minichromosome (fig. 2A, 3A).

Release of endogenous heterochromatin is required to enable silencing via tethered Clr4 methyltransferase

Although full length GBD-Clr4 protein is produced (fig. S1A) and recruited to *ura4::3xgbs-ade6*$^+$ (fig. S1D), it is unable to mediate silencing of this reporter. A possible explanation is that particular components of heterochromatin are limiting and thus when endogenous centromeric heterochromatin is intact there is insufficient protein available to allow the formation of robust silent heterochromatin at the ectopic site. Consistent with this, silencing of a centromeric marker gene is alleviated in cells expressing GBD-Clr4-∆cd fusion protein as the only source of Clr4 methyltransferase (fig. S2A), indicating that this heterochromatin is defective. Furthermore, deletion of the gene encoding the ribonuclease Dicer (*dcr1Δ*), which is essential for the generation of siRNA and thus RNAi, allows full length GBD-Clr4 protein to impose silencing on the *ura4::3xgbs-ade6*$^+$ reporter (fig. S2B). It is well known that *dcr1Δ* alleviates centromeric silencing and results in reduced H3K9 methylation and reduced binding of heterochromatin components. Thus a reasonable explanation is that the absence of RNAi releases components from endogenous heterochromatin allowing their recruitment by the action of full length GBD-Clr4 at the *ura4::3xgbs-ade6*$^+$ reporter to form silent

chromatin. This also supports our conclusion that the heterochromatin formed by tethering Clr4 activity does not require active RNAi.

Tethered GBD-Clr4-∆cd forms an extensive domain of silent chromatin.

When GBD-Clr4-∆cd is recruited to the *ura4::3xgbs-ade6*$^{+}$ reporter it forms an extensive domain of heterochromatin, as indicated by the accumulation of H3K9me2 and Swi6 over a domain of ~10 kb surrounding the 3xgbs tethering site (fig. 1B). RT-PCR analyses indicate that apart from the *3xgbs-ade6*$^{+}$ reporter, the adjacent *SPCC330.04c* and *SPCC330.06c* genes are also silenced (fig. S3). The promoters for *SPCC330.04c* and *SPCC330.06c* lie 4.7 kb and 2.6 kb, respectively, from the *3xgbs* tethering site. The extent of the silent chromatin formed at *ura4::3xgbs-ade6*$^{+}$ is similar to that formed by native centromeric repeat DNA placed at the *ura4* locus (*1*). The plasmids *p3xgbs-cc2* and *pcc2-3xgbs* also form a domain of synthetic heterochromatin when transformed into cells expressing GBD-Clr4-∆cd and this silences the adjacent marker genes (see below and fig. S7 and S8).

GBD-Clr4-∆cd mediated synthetic heterochromatin can be established *de novo* and maintained in the absence of active RNAi and Swi6

To determine if the heterochromatin formed by tethering GBD-Clr4-∆cd can be established *de novo* in the absence of RNAi, two strains lacking Dcr1 (*dcr1Δ::Nat*^{R}) were crossed (fig. S4A). Strain-I contained the *ura4::3xgbs-ade6*$^{+}$ reporter and is FOA resistant (FOA^{R}) because insertion of *3xgbs-ade6*$^{+}$ disrupts the *ura4* gene; Strain-II carries the hygromycin resistance gene closely linked to the modified *clr4* locus *GBD-clr4-Δcd* (*GBD-clr4-Δcd:Hyg*^{R}) and a wild-type *ura4*$^{+}$ locus (thus FOA sensitive). Hyg^{R} FOA^{R} progeny that express GBD-Clr4-∆cd and contain the *ura4::3xgbs-ade6*$^{+}$ reporter were selected. The majority of these formed red colonies on low adenine plates indicating that the *ura4::3xgbs-ade6*$^{+}$ reporter had established the silent state; few white expressing colonies were observed. qRT-PCR confirmed that *3xgbs-ade6*$^{+}$ was repressed in *dcr1Δ GBD-clr4-Δcd:Hyg*^{R} progeny and H3K9 methylation was readily detected on *3xgbs-ade6*$^{+}$ (fig. S4B). In a similar control cross between *ura4::3xgbs-ade6*$^{+}$ reporter and *GBD-clr4-Δcd:Hyg*^{R} strains lacking Rik1 (*rik1Δ::Nat*^{R}) no silencing was observed; all Hyg^{R}, FOA^{R} progeny formed white colonies, *3xgbs-ade6*$^{+}$ was expressed and H3K9me2 absent. Additional crosses of this type were performed with

pairs of strains lacking either Ago1, Chp1, Tas3, Chp2, or Swi6. Analyses of the resulting progeny indicated that synthetic heterochromatin can be efficiently established in the absence of the RNAi components Ago1, Chp1, Tas3 and the H3K9me binding chromo-domain protein Swi6, however, establishment is clearly dependent on the presence of Chp2, a paralog of Swi6 (fig. S4C).

Our analyses indicates that heterochromatin at *ura4::3xgbs-ade6*$^{+}$ locus can also be maintained largely independently of RNAi components Dcr1, Chp1, Ago1 and Tas3 and Swi6 whilst the maintenance of this silenced state is dependent on chromatin factors Rik1, Chp2, and the deacetylases Sir2 and Clr3 (fig. 1C, D). To quantify how efficiently this GBD-Clr4-Δcd mediated silencing is maintained upon removal of the genes encoding these proteins, crosses were performed between a wild-type strain in which the *ura4::3xgbs-ade6*$^{+}$ was silenced by GBD-Clr4-Δcd (Strain I; fig. S4C) and strains in which the gene of interest was deleted (*dcr1*Δ*, ago1*Δ*, tas3*Δ*, chp1*Δ*, rdp1*Δ*, rik1*Δ*, swi6*Δ*, chp2*Δ*, sir2*Δ*, clr3*Δ) that expressed GBD-Clr4-Δcd but lacked the *ura4::3xgbs-ade6*$^{+}$ reporter (Strain II). Analyses of progeny with the correct genotype from these crosses indicated that silencing is efficiently maintained (>93%) in the absence of RNAi components and Swi6 (fig. S4C). From the above analyses we conclude that RNAi components and Swi6 are not required for the *de novo* establishment or maintenance of silent synthetic heterochromatin over the *ura4::3xgbs-ade6*$^{+}$ reporter. In agreement with this, transformation of strains expressing GBD-Clr4-Δcd with plasmid DNA containing 3xgbs allowed establishment of H3K9me2 over the *3xgbs* region in wild-type and *dcr1Δ*, but not *rik1Δ* strains (fig. 3 and fig. S7).

Although *ura4::3xgbs-ade6*$^{+}$ transcript levels display some increase and H3K9me2 levels are somewhat reduced in *ago1*Δ*, tas3*Δ*, chp1*Δ cells (fig. 1C), no increase in transcription of or reduction in H3k9me2 on *ura4::3xgbs-ade6*$^{+}$ is observed in cells created by removal of Dcr1 (*dcr1Δ*; essential for the generation of siRNA) in synthetic heterochromatin maintenance assays. [Note: in establishment assays less H3K9me2 is apparent on the silent *ura4::3xgbs-ade6*$^{+}$ reporter (fig. S4B)]. Ago1, Tas3 and Chp1 associate to form the RITS complex which is recruited to H3K9me2 chromatin via the chromo-domain of Chp1. A plausible explanation is that the alleviation observed in *ago1*Δ*, chp1*Δ and *tas3*Δ*,* cells is due to their physical absence rather than a lack of RNAi directed events. In agreement with this, Ago1 was found to associate with the silent *ura4::3xgbs-ade6*$^{+}$ reporter (fig. S5C). In addition, no siRNA homologous silent reporter genes could be detected (fig. S5A, B); this is also consistent with the idea that

the process of RNAi does not actively participate in the GBD-Clr4-Δcd mediated silencing of *3xgbs-ade6*$^{+}$ and *3xgbs-ura4*$^{+}$ reporters. We conclude that RNAi components do not contribute in a substantial way to the formation of this synthetic heterochromatin and their contribution is as passive structural components rather than in mediating siRNA-dependent RNAi related events. If this were not the case, deletion of the gene encoding Dcr1 would be expected to affect synthetic heterochromatin to the same degree as deletion of those encoding the RITS components Ago1, Chp1 and Tas3 and the silent state would not be established in the absence of RNAi.

Synthetic heterochromatin formed by tethering Clr4 activity requires the presence of the known Clr4 substrate - lysine 9 of histone H3

The catalytically inactive GBD-Clr4-Δcd-H410K is unable to silence the *ura4::3xgbs-ade6*$^{+}$ reporter (fig. 1A). This indicates that Clr4 activity is required for the formation of GBD-Clr4-Δcd mediated synthetic heterochromatin and that it does not just result from the recruitment of a repressive complex via Clr4 interacting proteins. To determine if the known substrate of Clr4, lysine 9 of histone H3, is required we tested if the *ura4::3xgbs-ade6*$^{+}$ reporter could be silenced in cells expressing single copy of a histone H3 gene in which the lysine 9 residue was changed to arginine (H3K9R) or alanine (H3K9A). The *3xgbs-ade6*$^{+}$ reporter was clearly silenced in cells retaining only one wild-type histone H3 gene (H3.2) but silencing was lost in cells expressing H3K9R or H3K9A (fig. S6). This suggests the lysine 9 residue of histone H3 and methylation of lysine 9 is critical for the formation of this synthetic heterochromatin.

Extensive but distinct domains of H3K9me2 and CENP-A^{Cnp1} chromatin are formed on the plasmid-based circular minichromosomes

The *de novo* assembly of an active centromere on naïve DNA templates requires the presence of at least 2 kb of heterochromatic outer repeat and a central domain (*2*). To determine if synthetic heterochromatin is sufficient for this process, we substituted outer repeat heterochromatin with three Gal4-binding sites (3xgbs), by constructing the plasmid *p3xgbs-cc2*. The control plasmid *p0xgbs-cc2* has no Gal4-binding sites. Transformants containing these plasmids were selected in wild-type (*clr4*$^{+}$) cells or cells expressing GBD-Clr4-Δcd. ChIP analyses demonstrate that the GBD-Clr4-Δcd protein associates with the Gal4-binding sites on *p3xgbs-cc2* but not with the equivalent position of *p0xgbs-cc2*. Moreover, the same region of *p3xgbs-cc2*, but not *p0xgbs-cc2*, was

enriched in anti-H3K9me2 ChIP (fig. 2A). CENP-A^{Cnp1} and CENP-C^{Cnp3} only associate with *cc2* of *p3xgbs-cc2* in the presence of the GBD-Clr4-Δcd fusion protein and not with the central core of *p0xgbs-cc2* in the presence or absence of GBD-Clr4-Δcd (fig. 2B). To confirm and extend these findings, additional analyses were performed with the same and other primer-pairs (fig. S7A). The products assayed are located 2kb to the left of the 3xgbs tethering site (Product A; plasmid-his3$^+$ junction), the 3xgbs tethering site itself (product B), 2kb to the right of the 3xgbs tethering site (Product C; the *his3*$^+$*-cc2* junction), the middle of the central domain (Product D), a further 8.5 kb to the right of C (Product E; the *cc2-ura4*$^+$ junction). In addition primer pairs that detect two regions on the plasmid backbone 3.25 kb (Product G) and 4.5 kb (Product F) from the 3xgbs were also utilized. Again, we were able to detect H3K9me2 and kinetochore proteins (i.e. CENP-A/CENP-C) only on *p3xgbs-cc2* in cells expressing the fusion GBD-Clr4-Δcd. H3K9me2 was readily detected (fig. S7B, D) on the plasmid backbone (F,G) at the plasmid-*his3*$^+$ junction (A), the Gal4-binding sites (B) and at the *his3*$^+$*-cc2* junction (C), but was not detected in the middle of the central domain (D). In contrast, CENP-A^{Cnp1} and CENP-C^{Cnp3} were detected at the edges (C and E) and in the middle (D) of the central domain but were not detected over the Gal4-binding sites (B) (fig. S7 C, D). These analyses indicate that tethering of Clr4 methyltransferase to promotes the formation of a heterochromatin domain of at least 6 kb around the 3xgbs and this is sufficient to allow the assembly of CENP-A^{Cnp1} chromatin, including CENP-C^{Cnp3}, over a domain of approximately 8.5 kb encompassing the central core.

Synthetic heterochromatin forms mitotically active centromeres on plasmid-based minichromosomes in the absence of RNAi

To determine if plasmids assemble a functional centromere allowing mitotic segregation we utilised the red/white colony sectoring assay built into these plasmids (see SOM below). *p3xgbs-cc2*, but not *p0xgbs-cc2*, formed white colonies and only in cells expressing GBD-Clr4-Δcd (fig. 3C). A plasmid with Gal4-binding sites placed on the opposite side of cc2 (*pcc2-3xgbs*) gave similar results (fig. S9). Both *p3xgbs-cc2* and *pcc2-3xgbs* are more stable than *pH'-cc2*, a circular minichromosome which is of similar size containing one partial centromeric outer repeat. When *p3xgbs-cc2* was introduced into cells expressing GBD-Clr4-Δcd lacking Dcr1 (*dcr1D*) it still forms heterochromatin, assembles CENP-A^{Cnp1} chromatin on the central domain and exhibits mitotic stability as demonstrated by the appearance of white and white/red sectored colonies (fig. 3C and

S9). In contrast, the native outer repeat heterochromatin on *pH'-cc2* allows formation of a functional centromere in wildtype (white colonies - shown) but not in cells lacking Dcr1 (*2*).

Materials and Methods:

Strain and Plasmid Construction

Standard procedures were used for bacterial and fission yeast growth, genetics and manipulations (*4*). *S. pombe* strains used in this study are described in Table S1. Primer sequences are listed in Table S2. Cells were grown at 32^{o}C in all the experiments unless indicated otherwise. All additional details on strain construction and primer sequences are available on request. FY10391 (*GBD-clr4*$^{+}$) and FY9669 (*GBD-clr4-Δcd*) were derived from FY8628. To construct FY8628 the *ura4*$^{+}$ marker was inserted into the *clr4* locus (5' region of the *clr4* gene) of FY1180, which has a silent *ade6*$^{+}$ marker gene integrated in the outer repeat of cen1 (*cen1-otr(Sph1):ade6*$^{+}$) (*3*). This *ura4*$^{+}$ marker was replaced with the hybrid GBD-clr4^{+} or GBD-clr4-Δcd construct. These hybrid PCR constructs were made using a plasmid containing the Gal4 DNA binding domain (GBD) ORF (Matchmaker Kit, Clontech) and genomic DNA from either wild-type *clr4*$^{+}$ or *clr4-Δcd* strains (FY8630 that has *clr4* gene sequence lacking the part encoding for the chromo domain: Δ19-180 in relation to +1 of *clr4*$^{+}$ ORF DNA sequence or Δ7-59 amino acid residues of Clr4 protein, respectively).

To create the FY10084 and FY10473 strains, the Hygromycin B resistance marker (HphMX6) was integrated 1 kb upstream of the *clr4*$^{+}$ ORF start site in the strains FY9863 and FY10391 respectively. HphMX6 cassette was amplified from pFA6a-HphMX6 plasmid (*5*).

To construct the FY10676 (*GBD-clr4-H410K-Δcd*) strain, first the *ura4*$^{+}$ marker was introduced in FY10303 strain to disrupt the 3' region of the *clr4* gene. The resulting strain was then transformed with *clr4* mutant PCR construct (substitutions C1228A, C1230A; H410K) to replace *ura4*$^{+}$ and create *clr4-H410K-Δcd*. The resulting strain was modified to insert the CloNat resistance cassette (NatMX6) 1 kb upstream, as described above for the HphMX6 cassette, using same primers and pFA6a-NatMX6 (*3*) as template.

FY8676 strain was constructed by disrupting the *ura4*$^{+}$ gene in FY8674 strain using a modified version of pBW5/6 (kind gift from K. Scott), called pBW5/6-3xgbs. Digestion with *Pst*I, allowed integration of *ade6*$^{+}$ with *ade6* promoter and three tandem GAL4 UAS

sequences (*3xgbs*) upstream of the promoter into the *ura4* ORF. pBW5/6-3xgbs plasmid was constructed by ligating 3 tandem GAL4 UAS sequences (TCGACGGAGGACAGTCCTCCG) into the *Bgl*II site of the pBW5/6 plasmid.

FY10126 (*10xgbs-ura4*$^+$) strain was constructed as follows. FY8676 strain was transformed with the hybrid *10xgbs-ura4* fragment to replace the *3xgbs-ade6*$^+$ with the array containing 10 tandem Gal4 UAS sequences (TCGGAGGACAGTACTCCGC), resulting in a reconstruction of the *ura4*$^+$ locus, where 10xgbs array are inserted at position -114 relative to *ura4* start site (+1). *Ura*$^+$ *ade6*$^-$ transformants were selected, and integrity of the *10xgbs-ura4*$^+$ locus was confirmed by sequencing.
To make strains FY10524, and FY10525, the Hygromycin B resistance marker was integrated 360 bp downstream of the H3.2 ORF stop site in the strains FY6072 and FY6068, respectively, and then appropriate crosses were performed.
FY12146 strain was constructed as follows. FY1555 strain was transformed with a hybrid *ura4-GFP* construct to make FY8090 strain. FY12110 strain was constructed from the strain FY8090 via the same manipulation as FY8676 out of FY8674 (as described above), and appropriate crosses were performed thereafter to make FY12146 strain.
The construction of strains with an insertion of a non-functional *his3* gene inserted at *cc2* (*cc2:his3*) was previously described (*2*). For simplicity, in this study, pSp-cc2+K" (*6*) is referred as *pH'-cc2*. *p0xgbs-cc2* was obtained by releasing the 2.1 kb *Kpn*I fragment containing *otr* from *pH-cc2* (*2*). For the construction of the plasmids *p3xgbs-cc2* and *pcc2-3xgbs*, a 0.4 kb fragment containing *3xgbs* was excised from pBW5-3Gal with *Bgl*II and ligated to the *Bgl*II unique site at *p0xgbs-cc2* giving as a result *p3xgbs-cc2*. Otherwise, a 1.5 kb fragment containing 3x*gbs* was excised from pBW5-3Gal with *Spe*I and *Xba*I and ligated to *p0xgbs-cc2*, previously digested with *Avr*II, producing *pcc2-3xgbs*.

ChIP: Chromatin Immunoprecipitation

In all the cases cells were grown at 32^{o}C. ChIP was performed as described (*7*) except for the following modifications. For H3K9me2, GBD, Cnp1 and Cnp3 ChIPs, cells were fixed in 1% PFA for 15 min at room temperature. For Ago1-Flag and Swi6 ChIPs, cells were incubated for 2hr at 18^{o}C prior to fixing in 3% PFA for 30 min at room temperature. For H3K9me2 and GBD ChIPs cells were lysed using a bead beater (Biospec products) and the chromatin was sheared using a Bioruptor (Diagenode) sonicator (15 min of 30s

ON and 30s OFF on 'high' [200 W] power). For Ago1-Flag, Swi6, Cnp1 and Cnp3 ChIPs, cells were lysed by incubation with 0.4 mg/ml Zymolyase 100T (ICN) for 30 min at 37°C. 1μl of monoclonal H3K9me2 antibody (m5.1.1) (*8*), 10μl of polyclonal Swi6 antibody (*9*), 2.5μl of polyclonal GAL4 antibody (Covance, #PRB-255C), 10ul of polyclonal Cnp1 (*10*), 10ul of polyclonal Cnp3 (*2*) antibody were used per ChIP. For Ago1-Flag 25μl of M2 EzView resin (Sigma) was used per ChIP. Competitive duplex PCR was perfomed to analyse ChIP samples using oligonucleotides specific to the regions of interest and to the control gene *fbp1* (Table S2). Each Input sample (T=total) was diluted 100 fold to provide comparable band intensity with the matching resuspended immunopreciptate (IP). The PCR programme used was 94°C for 4 minutes followed by 30 cycles of 94°C for 30 seconds, 55°C for 30 seconds and 72°C for 1 minute with a final step of 5 minutes at 72°C. The PCR products were run on 1.5% TBE-agarose gels, stained with ethidium bromide 10 μg/ml and the quantitated using the Kodak EDAS 290 system and 1D Image Analysis Software (Eastman Kodak). ChIP enrichment of a chromosomal region of interest (*3xgbs*, *cc1/3*, *cc2*, *otr*, *ade6*$^+$, and fig S7 primer pairs A, B, C, D, E, F, G) was calculated relative to the control *fbp1* product, and then corrected for the ratio obtained in the input (T) sample. Some variation in fold-enrichments was observed, however, the pattern of enrichment versus no-enrichment was consistent between experiments. Representative examples are shown. For each experiment presented, 2-6 independent transformants or progeny (from crosses) were analysed and ChIP performed at least three times.

qPCR

Real-time PCR (qPCR) was performed using 2x SYBR Green Jumpstart Mix (Sigma) on a Bio-Rad iCycler. PCR reactions were set up with standard quantities of oligos and template and monitored by fluorescence reading throughout the following programme: 95°C for 2 minutes followed by 45 cycles of 95°C for 15 seconds, 50°C for 30 seconds and 72°C for 30 seconds. Primers used for real-time PCR are listed in Table S2. Data was recorded and analyzed using iCycler iQ Optical System Software v3.0a and Microsoft Excel. Each sample was analyzed in triplicate. The performance of all oligo pairs was evaluated in a dilution series of template DNA (5 fold, minimum of 5 points). The PCR amplification efficiency of each pair was then calculated from the resulting standard curve using the following formula: E = 10^(-1/slope) where E is efficiency and slope is obtained from the regression equation (R^2≥0.990). Ratios were calculated from

average threshold cycle values using the Pfaffl method of relative quantification: ratio = E_{target}^($Ct_{reference}$ – $Ct_{subject}$) / $E_{control}$^($Ct_{reference}$ – $Ct_{subject}$), where E is efficiency of either target or internal control PCR and Ct is threshold cycle for reference or subject samples (*11*). Histograms represent the average results of at least three independent experiments with error bars representing standard deviation.

RNA analysis

Large RNA for RT-PCR was obtained by using RNeasy Mini Kit (Qiagen). RT samples were prepared with random hexamers and Superscript III (Invitrogen) following manufacturer's instructions and then analysed by qPCR. Small RNA was obtained by resuspending cells in 50 mM Tris–HCl pH 7.5, 10 mM EDTA pH 8, 100 mM NaCl, 1% SDS, lysing by the addition of phenol:chloroform 5:1 and acid washed beads and then vortexing for 30 min at 4°C. The soluble fraction was extracted with phenol/chloroform. Large RNA was precipitated with 10% polyethylene glycol 8000 and 0.5 M NaCl on ice for 30 min followed by centrifugation. Small RNA was precipitated from the supernatant by addition of ethanol and sodium acetate, incubation at -20°C o/n, and followed by centrifugation. sRNA was run on an 12% polyacrylamide gel. sRNA gels were blotted by semi-dry electro transfer onto Hybond-NX membrane (GE Healthcare) and UV crosslinked. sRNA membranes were probed with ^{32}P-labeled oligos or PCR product. For cen-dh/dg siRNA analysis the probe was a mixture of three labeled oligos complementary to *dh* and *dg* repeats (IK8, IK9 and IK10). For ura4 siRNA analysis a 1.8 kb HindIII fragment containing the ura4 ORF and surrounding genomic DNA sequence was used. For *ade6* siRNA analysis a PCR product was used produced with the primers ADE6_FW and ADE6_RV. For the loading control a labeled oligo complementary to snRNA58 was used.

Protein immunoprecipitation and Western analyses

For the protein preparations for each sample, 1 g of cells, lysed using a bead beater (Biospec products), was used. Immunoprecipitations were performed using 20 μL (1:100 dilution) polyclonal antibody against GAL4 protein DNA binding domain (Covance) coupled to protein A agarose (Pharmacia) for 90 minutes. After washes, proteins were eluted with hot loading buffer, separated on 4-12% Nupage SDS-PAGE gel (Invitrogen), and subjected to a western blot using monoclonal antibody against GAL4 protein DNA binding domain (Clontech). Control western blot was performed using

monoclonal antibody against tubulin (kind gift from Keith Gull).

***S. pombe* plasmid manipulations**

Cells were grown at 32^{o}C in all the experiments involving minichromosomes (e.g. ChIP, spotting assay, minichromosome loss assay). Plasmids *pH'-cc2*, *p3xgbs-cc2*, *pcc2-3xgbs* and *p0xgbs-cc2* were introduced into *S. pombe* by electroporation and transformants were selected by growth on PMG –ura –ade for 5-7 days with the exception of *pcc2-3xgbs*, which was selected on PMG –his.

In ChIP experiments, a plasmid stability test was performed at the time of fixation in order to confirm that plasmids were behaving episomally and had not integrated (*2*). In order to check the integrity of the plasmid DNA in *S. pombe*, Southern blots were performed as described (*2*). 2-10 µg of DNA were digested overnight with 40-80U of *BamH*I and *Xba*I (NEB). Samples were run on 0.4% SeaKem Gold agarose (Cambrex Biosciences, Rochester, USA) in 1X TAE buffer. A 607 bp *his3* probe from *pH-cc2* (*2*) was used as probe in the hybridisations.

Testing mitotic stability of plasmid based minichromosomes

To determine if plasmids can assemble a functional centromere allowing mitotic segregation we utilised a red/white colony colour assay built into these plasmids. *sup3-5* suppresses the ade^{-}/red *ade6-704* allele, rendering these cells ade^{+} and white colony forming. A mitotically stable *sup3-5*-containing circular minichromosome with a functional centromere will form white colonies, while plasmid loss results in red colonies. A sectoring assay accurately measures the rate of mini-chromosome loss per cell division (*3*). Colonies that are half or less than half white are derived from a cell that initially contained the plasmid; plasmid missegregation in the first division results in its loss from one cell which forms a red sector, the sister cell retaining it forms the white sector. Loss in successive division results in a white sector occupying 50%, 25%, 12.5% or less of a colony.

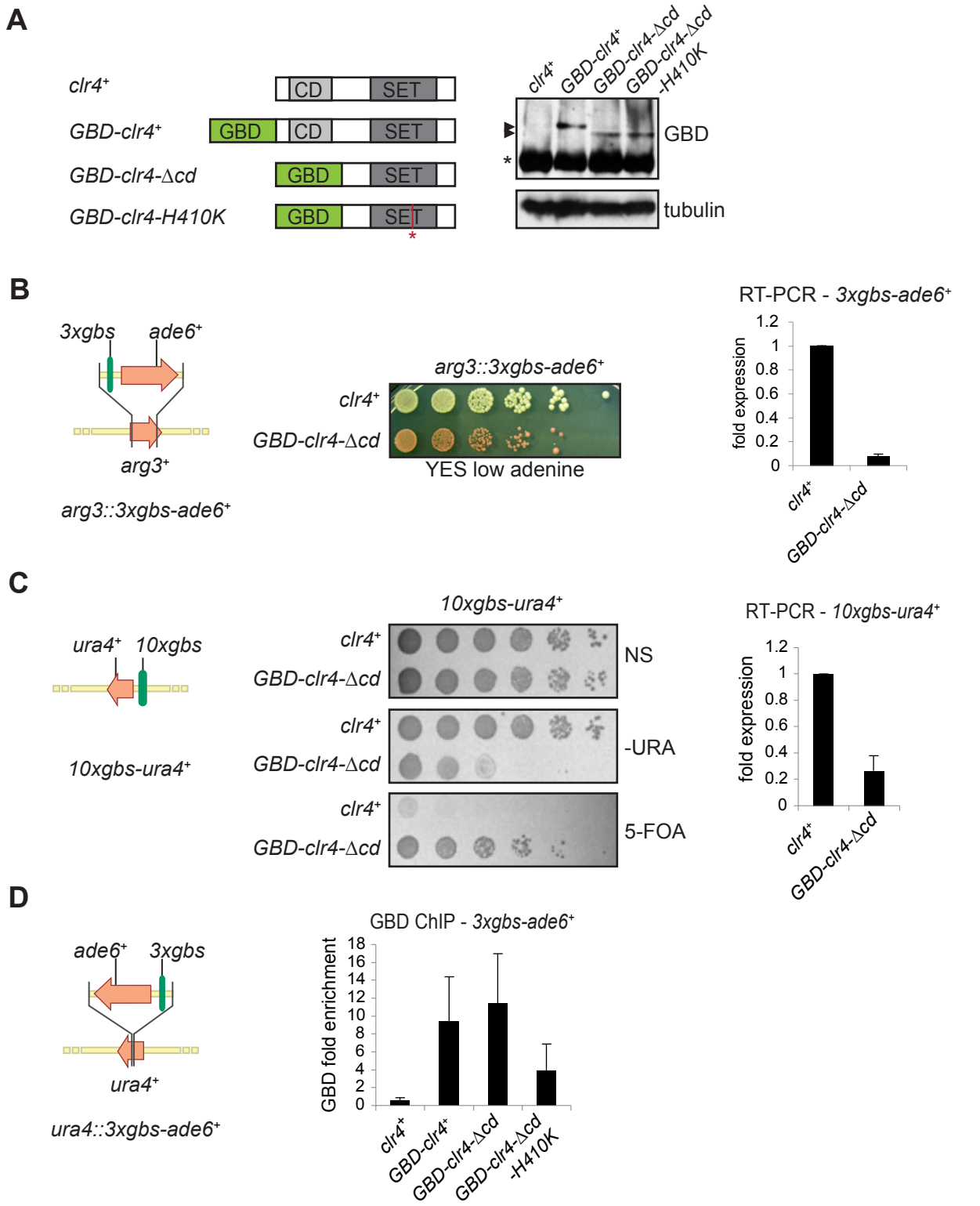

Figure S1. GBD-Clr4-Δcd is recruited to *3xgbs* and silences *gbs* reporters inserted at *arg3*$^+$ and *ura4*$^+$ loci.**(A)** Left: Diagram depicting Clr4 fusion proteins used. CD, chromodomain; SET, SET methyltransferase domain; GBD, Gal4 DNA binding domain; *red*, position of H410K point mutation. Right: Western analyses of α-GBD immunoprecipitates showing levels of indicated Clr4 proteins. Loading control: α-tubulin western of initial lysate samples.**(B)** Left, diagram of *arg3::3xgbs-ade6*$^+$ reporter. Middle, plating assay on low adenine of *arg3::3xgbs-ade6*$^+$ containing cells expressing the indicated Clr4 proteins. Wild-type *ade6*$^+$ expressing cells form white colonies; *ade*$^-$*/ade6*$^+$ repressed cells form red colonies. Right, qRT-PCR showing *3xgbs-ade6*$^+$ transcript levels (error bar is SD, n=3). **(C)** Left, diagram of *10xgbs-ura4*$^+$ reporter. Middle, growth assay of cells with *10xgbs-ura4*$^+$ expressing Clr4 or GBD-Clr4-Δcd on non-selective (NS), -URA and 5-FOA plates. Right: qRT-PCR showing *10xgbs-ura4*$^+$ transcript levels in non-selective media (Error bar: SD, n=3). **(D)** Left, diagram of *ura4::3xgbs-ade6*$^+$ reporter. Right, qChIP showing levels of GBD-Clr4 proteins bound to 3xgbs (Error bar: SD, n=3).

Kagansky et al. Figure S1

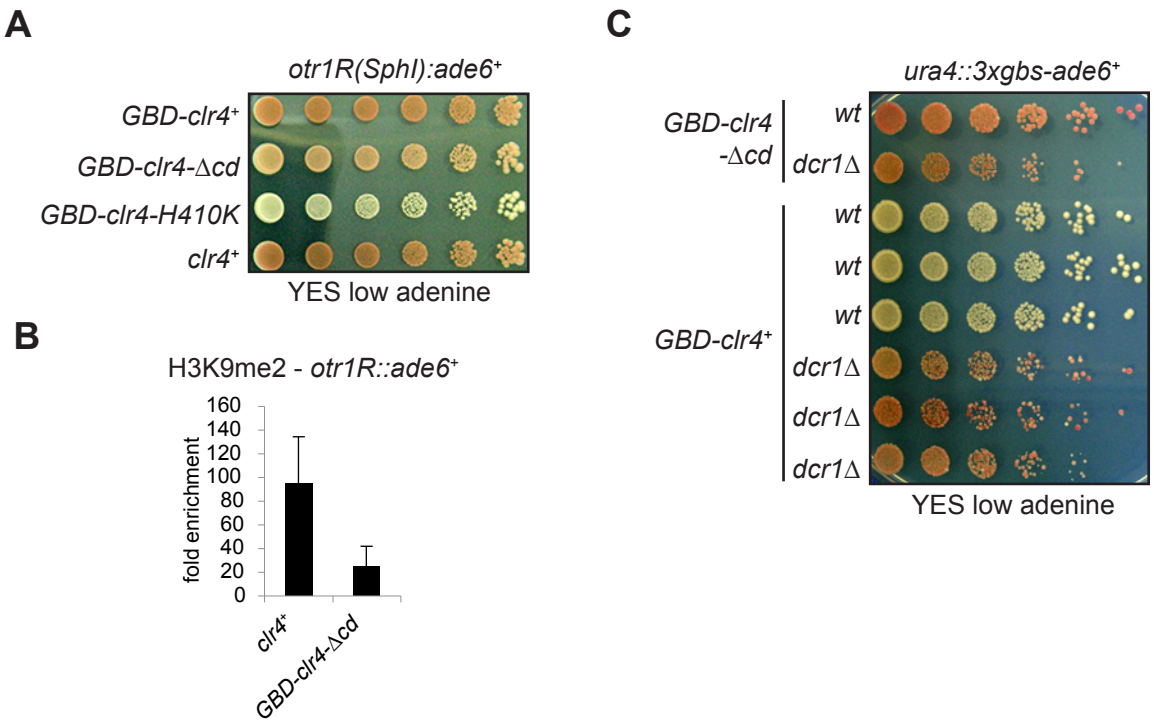

Figure S2 – Weakened centromeric heterochromatin facilitates silencing at the 3xgbs tethering site.
(**A**) Deletion of the Clr4 chromo-domain alleviates endogenous centromeric outer repeat silencing. Cells containing the *ade6*$^+$ gene inserted in centromeric heterochromatin [*otr1R(SphI):ade6*$^+$] and expressing the indicated Clr4 proteins were plated on low adenine media. (**B**) qChIP showing levels of H3K9me2 over *otr1R(SphI)::ade6*$^+$ in cells expressing the indicated Clr4 proteins (error bar is SD, n=3). (**C**) Dicer allows full length GBD-Clr4 to silencing of the *3xgbs-ade6*$^+$ reporter. Plating assay on low adenine of *ura4::3xgbs-ade6*$^+$ containing cells expressing the indicated Clr4 proteins in the presence (*wt*) or absence of Dcr1 (*dcr1*Δ).

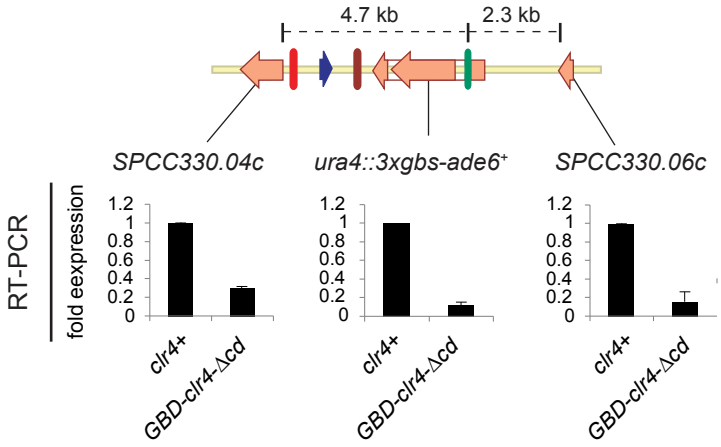

Figure S3 – Heterechromatin assembled by GBD-Clr4-Δcd represses transcription of nearby genes.
qRT-PCR showing *3xgbs-ade6*$^{+}$ and adjacent gene transcript levels in presence of Clr4 or GBD-Clr4-Δcd (Error bar: SD, n=3).

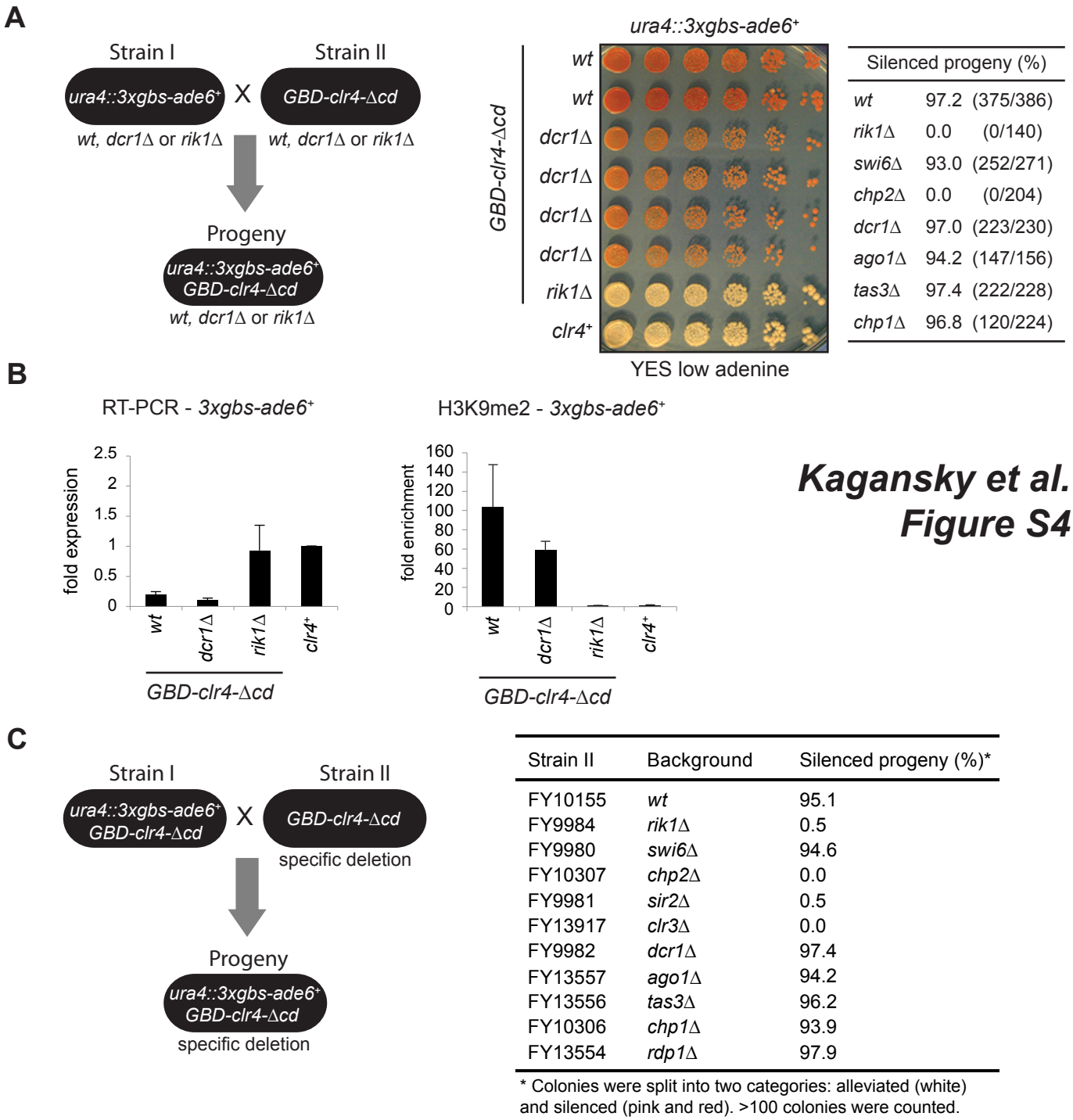

Strain II	Background	Silenced progeny (%)*
FY10155	*wt*	95.1
FY9984	*rik1*Δ	0.5
FY9980	*swi6*Δ	94.6
FY10307	*chp2*Δ	0.0
FY9981	*sir2*Δ	0.5
FY13917	*clr3*Δ	0.0
FY9982	*dcr1*Δ	97.4
FY13557	*ago1*Δ	94.2
FY13556	*tas3*Δ	96.2
FY10306	*chp1*Δ	93.9
FY13554	*rdp1*Δ	97.9

* Colonies were split into two categories: alleviated (white) and silenced (pink and red). >100 colonies were counted.

Figure S4. Factors required for establishment and maintenance of silencing by GBD-Clr4-Δcd.
(A) Diagram of heterochromatin establishment assay. Pairs of strains carrying the *ura4::3xgbs-ade6*$^+$ reporter (I) or the *GBD-clr4-Δcd* (II) were crossed. The progeny from paired *wt*, *dcr1*Δ or *rik1*Δ crosses were analysed for their ability to establish heterochromatin de novo on *ura4::3xgbs-ade6*$^+$ via GBD-Clr4-Δcd. Right, plating assay on low adenine plate of progeny cells of indicated genotype from IxII establishment assays. Quantification of de novo establishment assays performed in strains as indicated. The values illustrate the fraction of progeny in which silencing was established (colony counts in brackets). Spores were plated onto media with limiting adenine and the resulting colonies were classified according to colour. **(B)** Left, qRT-PCR for *3xgbs-ade6*$^+$ transcript levels in progeny cells of indicated genotype from establishment assay in B (Error bar: SD, n=3). Right, qChIP for H3K9me2 levels on *ura4::3xgbs-ade6*$^+$ in the indicated progeny (Error bar: SD, n=3). **(C)** Left, Diagram highlighting the cross strategy for maintenance of silencing. Strain I, containing a silent copy of *ura4::3xgbs-ade6*$^+$, was crossed to Strain II that carried *GBD-clr4-Δcd* and was *wt* or had the indicated gene deleted. The selected progeny was then scored for silencing. Right, results for maintenance of *ura4::3xgbs-ade6*$^+$ silencing in the progeny of crosses with wild-type or specific gene deletion strains. Quantification of maintenance was as in A. The values illustrate the fraction of progeny in which silencing was maintained in the absence of the indicated genes (colony counts in brackets).

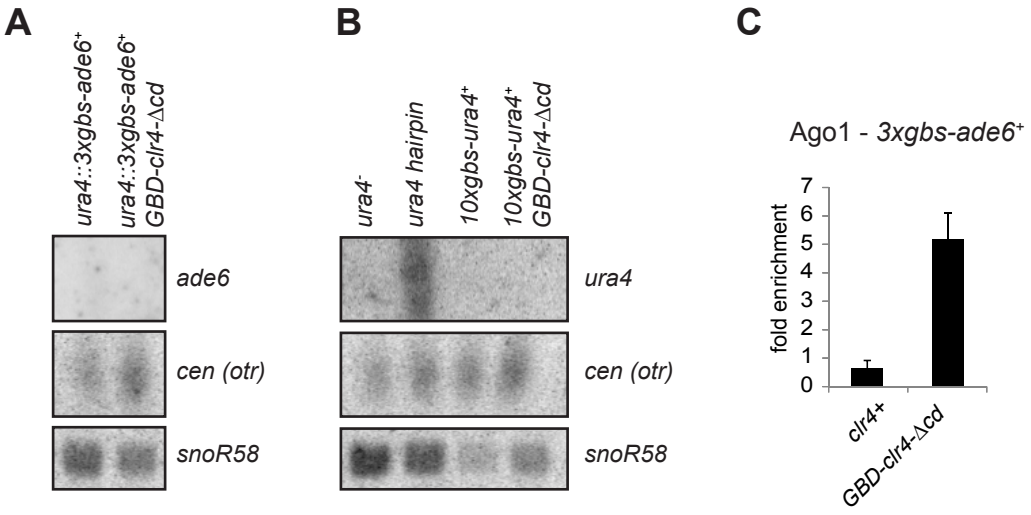

Figure S5 – No siRNAs are detectable for marker genes silenced by GBD-Clr4-Δcd
(**A**) Northern analysis of low molecular weight fraction of total RNA extracted from cells containing *ura4::3xgbs-ade6*$^{+}$. The membrane was probed for *ade6* ORF, centromeric *otr* (*dg*, positive control) and *snoR58* (loading control). (**B**) Similar analysis as in A. using cells containing *10xgbs-ura*$^{+}$. The positive control for *ura4* siRNAs is provided from cells expressing a hairpin construct which generates *ura4* siRNAs. (**C**) Ago1 associates with the silenced *3xgbs-ade6*$^{+}$ reporter. Cells containing *ura4::3xgbs-ade6*$^{+}$ and expressing FLAG-Ago1 in the presence or absence of GBD-Clr4-Δcd were processed for ChIP. qPCR analyses indicated that FLAG-Ago1 is enriched over *3xgbs-ade6*$^{+}$ when silenced by the presence of GBD-Clr4-Δcd. (Error bar: SD, n=3).

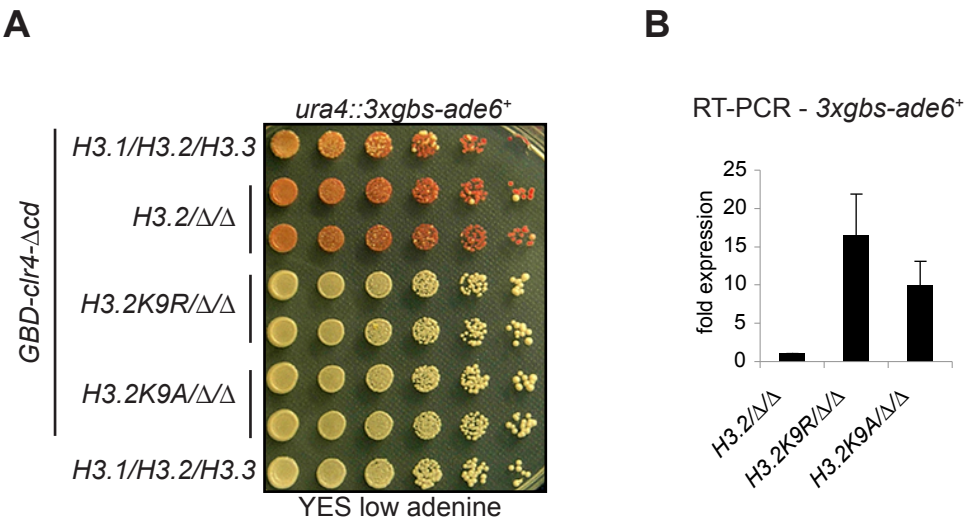

Figure S6. Histone H3 lysine 9 is required for GBD-Clr4-Δcd mediated heterochromatin
(A) Plating assay on low adenine of cells expressing GBD-Clr4-Δcd together with a single copy of histone H3 (H3.2/Δ/Δ) with the indicated mutations (H3.2K9R/Δ/Δ and H3.2K9A/Δ/Δ).
(B) qRT-PCR showing *3xgbs-ade6*$^{+}$ transcript levels in the presence of GBD-Clr4-Δcd in the wild-type (H3.2/Δ/Δ) relative to the mutants H3.2K9R/Δ/Δ and H3.2K9A/Δ/Δ (error bar is SD, n=3).

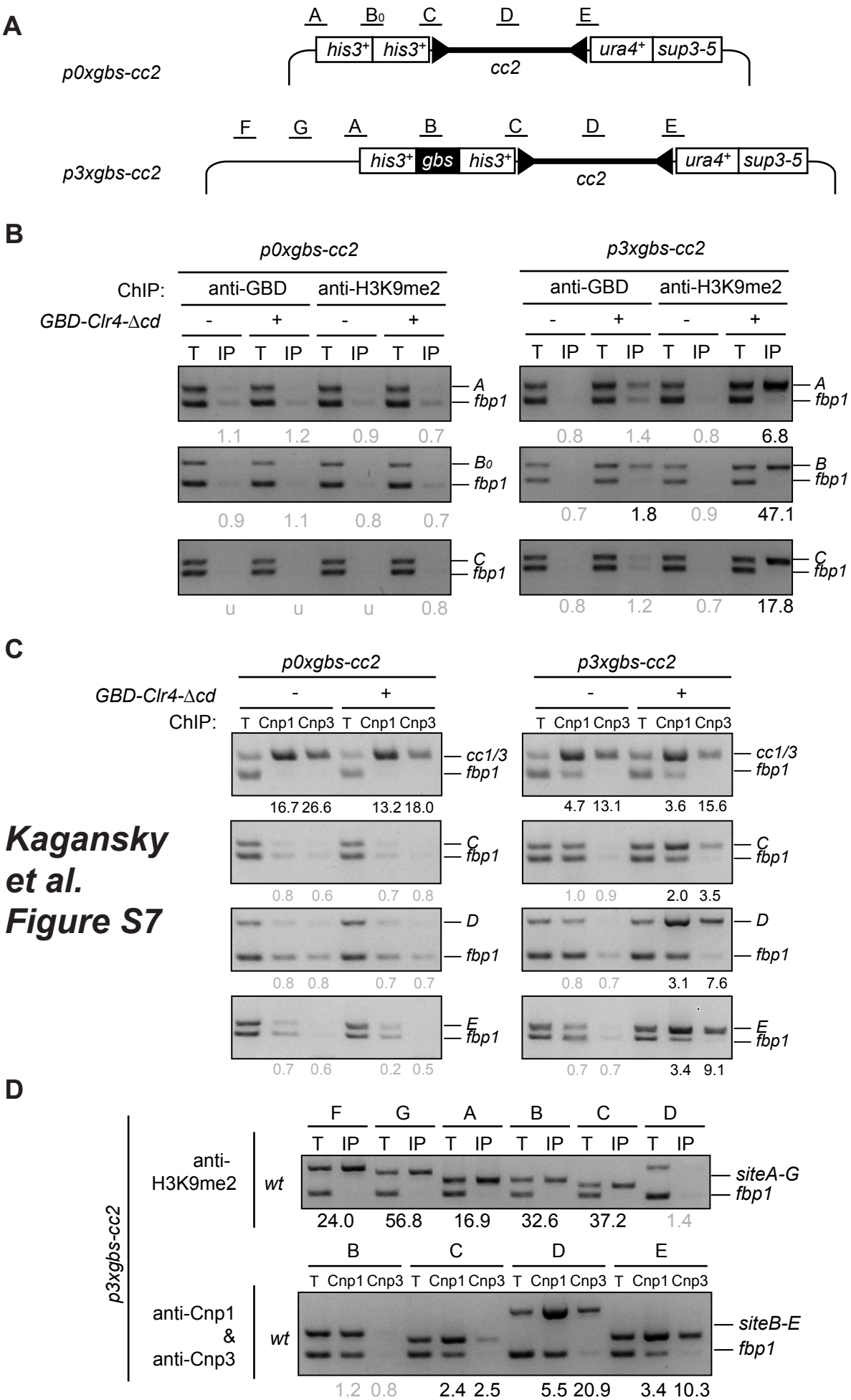

Kagansky et al. Figure S7

Figure S7. Tethered Clr4 promotes H3K9me2 deposition, kinetochore assembly and centromere activity**.**
(A) Diagram of plasmids used. *p0xgbs-cc2* and *p3xgbs-cc2* contain zero (0x*gbs*) or 3 Gal4 sites (3x*gbs*) and a central domain from cen2 (cc2).The plasmids also contain the *sup3-5* marker, which suppresses ade-/red *ade6-704* allele. Regions (A-E) analysed in ChIP by PCR are indicated. **(B)** ChIP with anti-GBD and anti-H3K9me2 of *wt* and *GBD-clr4-*Δ*cd* cells transformed with *p0xgbs-cc2* or *p3xgbs-cc2* as indicated. Enrichment values (IP/T) were calculated from the intensity of the plasmid bands normalized to the control *fbp1* locus. Grey values indicate no enrichment. For those marked 'u', PCR bands were undetectable. **(C)** ChIP with anti-Cnp1 and anti-Cnp3 of *wt* and *GBD-clr4-*Δ*cd* cells transformed with *p0xgbs-cc2* or *p3xgbs-cc2* as shown in B. Levels on endogenous centromeric *cc1/3* sequences are shown (top). **(D)** H3K9me2 and CENP-A^{Cnp1} chromatin occupy substantial and distinct domains at functional centromeres formed on plasmid-based minichromosomes by recruitment of Clr4 methyltransferase. ChIP with anti-Cnp1 and anti-Cnp3 (bottom) and anti-H3K9me2 (middle) of various *GBD-clr4-*Δ*cd* cells transformed with *p3xgbs-cc2*. PCR product positions are indicated (top). While kinetochore proteins are enriched at the central domain (C, D, E), H3K9me2 spreads over adjacent *his3* genes and plasmid backbone regions (A (2 kb from Gal4 sites), B, C (2 kb), G (3.25 kb), F (4.5 kb)). Enrichment values (IP/T) were calculated from the intensity of the plasmid bands normalized to the control *fbp1* locus. Grey values indicate no enrichment.

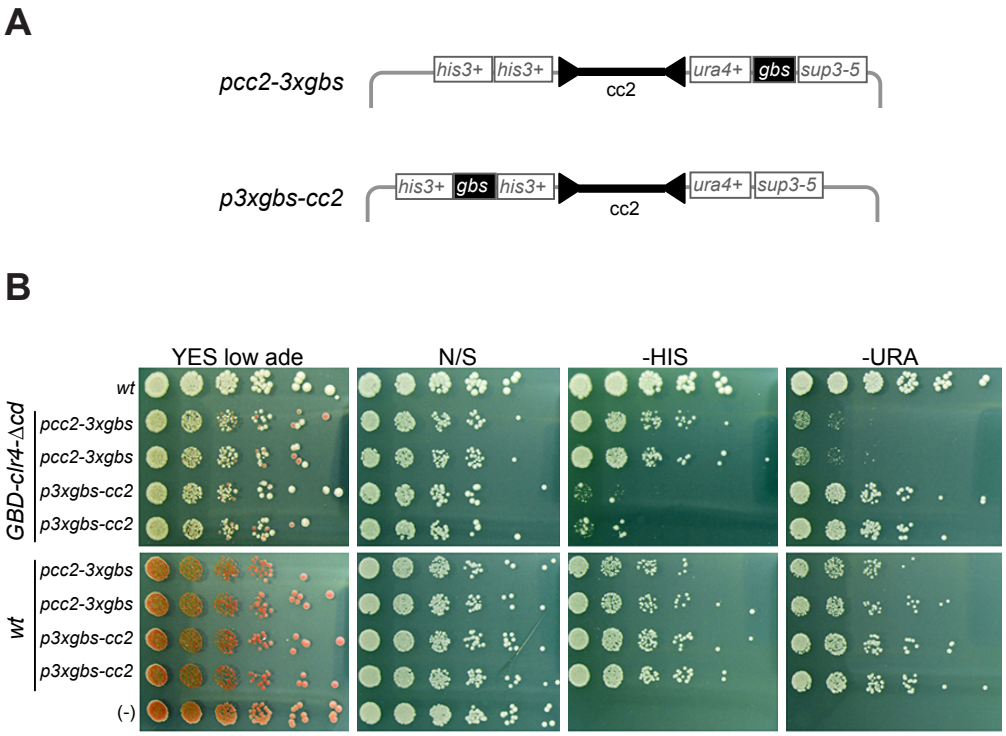

Figure S8 – Tethering Clr4 to plasmid DNA silences adjacent genes
(A) Diagram of the plasmids used on this assay, created by inserting the *3xgbs*(as indicated) on the left or right sides of the central core sequence (cc2) within copies of *his3*$^{+}$ or adjacent to *ura4*$^{+}$ marker genes, respectively. **(B)** *GBD-clr4-Δcd* and wild type cells containing either *pcc2-3xgbs* or *p3xgbs-cc2* were grown in liquid culture and plated in serial dilution on YES low adenine plates to indicate minichromosome stability (i.e. red colonies: unstable/lost; white/sectored colonies: stable/retained). PMG (minimal medium) containing full supplements (N/S) or lacking either histidine (-HIS) or uracil (-URA). Poor growth on –HIS or –URA indicates that the his3+ or ura4+ genes are silenced by the expression of GBD-clr4-Δcd. Prototroph (wt) and auxotroph (-) strains are included as controls.

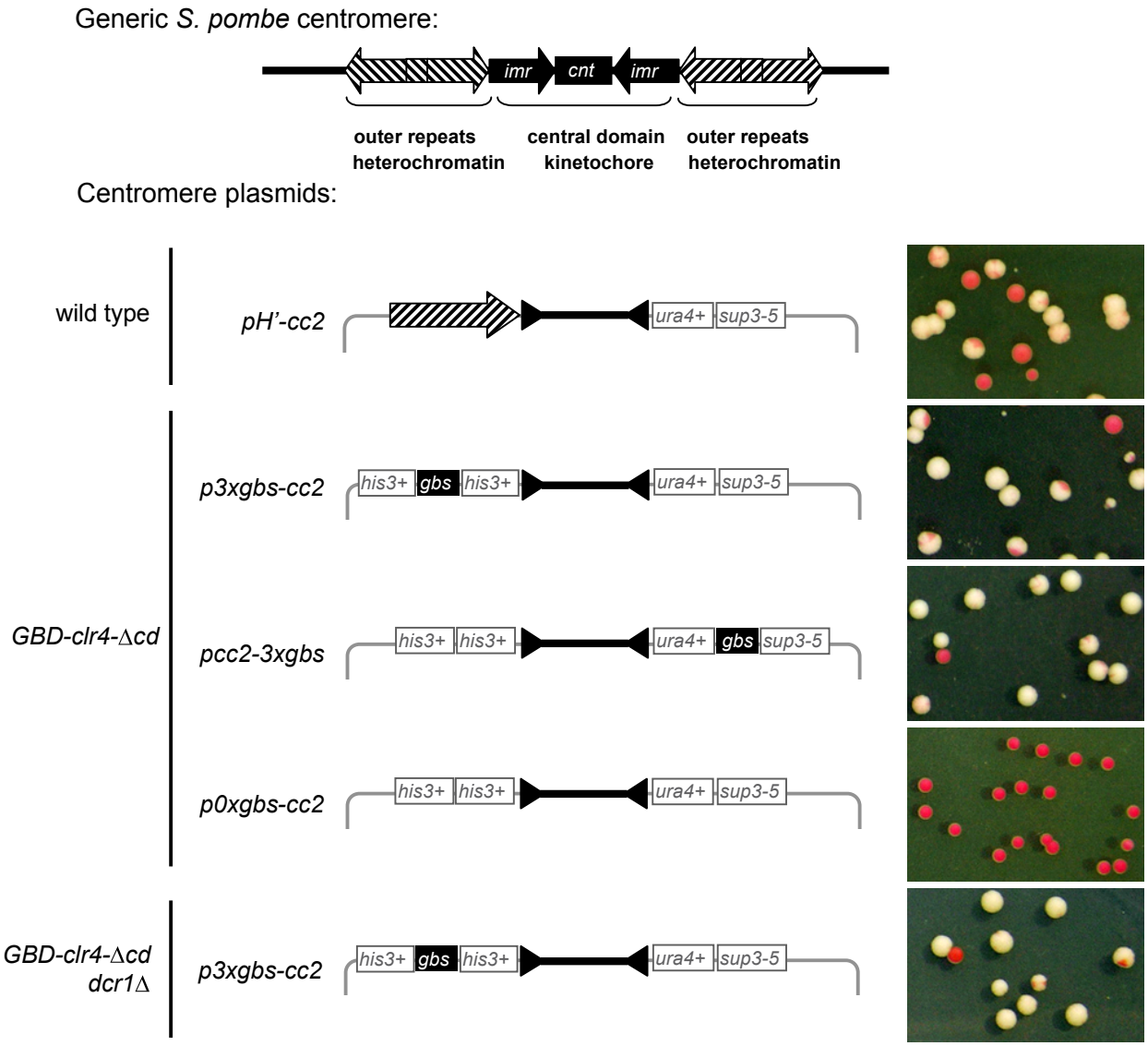

Figure S9. Synthetic heterochromatin provides equivalent centromere function as native heterochromatin on plasmid-based minichromosomes, even in the absence of Dicer.
Diagram of fission yeast centromere DNA and plasmids utilised (left). Examples of colonies formed in half-sector plating assay used to measure minichromosome loss rate (see Fig 3C and Method above) are shown (right). *pH'-cc2* contains a 2 kb portion of a centromeric outer repeat and forms a functional centromere.

Table S1. List of Strains Used in This Study

Strain	Genotype
FY199	*h⁻ leu1-32*
FY1555	*h⁺ his3-D1 leu1-32 ura4-D18 ade6-210*
FY1646	*h⁺ ade6-210 arg3-D4 his3-D1 leu1-32 ura4-D18*
FY7591	*h⁺ ade6-704 arg3-D4 his3-D1 leu1-32 ura4-DSE cc2:his3*
FY8090	*h⁺ arg3::ura4-GFP his3-D1 leu1-32 ura4-D18 ade6-210*
FY8628	*h⁺ clr4Δ(-198,+203) ade6-210 otrISphI:ade6⁺ ura4-D18*
FY8630	*h⁺ clr4-Δcd ade6-210 otrISphI:ade6⁺ ura4-D18*
FY8637	*h⁺ clr4Δ(+2201,+2429) ade6-210 otrISphI:ade6⁺ ura4-D18*
FY8674	*h⁻ ade6-DN/N his3-D1*
FY8675	*h⁺ ura4::3gbs-ade6⁺ ade6-DN/N his3-D1*
FY8676	*h⁻ ura4::3gbs-ade6⁺ ade6-DN/N his3-D1*
FY9669	*h⁺ GBD-clr4-Δcd ade6-210 otrISphI:ade6⁺ ura4-D18*
FY9863	*h⁹⁰ GBD-clr4-Δcd ura4::3gbs-ade6⁺ ade6-DN/N*
FY9932	*h⁻ 3xFlag-ago1-KanMX6, ade6-210, arg3D, his3D, leu1-32, ura4-D18*
FY9980	*h⁻ swi6::NatMX6 GBD-clr4-Δcd ade6-DN/N*
FY9981	*h⁹⁰ sir2::NatMX6 GBD-clr4-Δcd ade6-DN/N leu1-32*
FY9982	*h⁻ dcr1::NatMX6 GBD-clr4-Δcd ade6-DN/N leu1-32*
FY9984	*h⁻ rik1::KanMX6 GBD-clr4-Δcd ade6-DN/N leu1-32*
FY10084	*h⁹⁰ GBD-clr4-Δcd-HphMX6 ura4::3gbs-ade6⁺ ade6-DN/N*
FY10126	*h⁻ ura4::10gbs-ura4⁺ ade6-DN/N his3-D1*
FY10155	*h⁻ GBD-clr4-Δcd-HphMX6 ade6-DN/N his3-D1*
FY10301	*h⁺ ura4::10gbs-ura4⁺ ade6-DN/N his3-D1 leu1-32 GBD-clr4-Δcd-HphMX6*
FY10302	*h⁻ ura4::10gbs-ura4⁺ ade6-DN/N his3-D1 GBD-clr4-Δcd-HphMX6*
FY10303	*h⁺ GBD-clr4-Δcd-HphMX6 ura4::3gbs-ade6⁺ ade6-DN/N*
FY10306	*h⁻ chp1::KanMX6 GBD-clr4-Δcd-HphMX6 ade6-DN/N leu1-32*
FY10307	*h⁹⁰ chp2::KanMX6 GBD-clr4-Δcd-HphMX6 ade6-DN/N leu1-32*
FY10356	*h⁻ GBD-clr4-Δcd-NatMX6 ura4::3gbs-ade6⁺ ade6-DN/N*
FY10391	*h⁺ GBD-clr4⁺ ade6-210 otrISphI:ade6⁺ ura4-D18*
FY10404	*h⁻ rdp1::NatMX6 GBD-clr4-Δcd-HphMX6 ura4::3gbs-ade6⁺ ade6-DN/N*
FY10405	*h⁻ tas3::KanMX6 GBD-clr4-Δcd-HphMX6 ura4::3gbs-ade6⁺ ade6-DN/N*
FY10407	*h⁻ ago1::KanMX6 GBD-clr4-Δcd-HphMX6 ura4::3gbs-ade6⁺ ade6-DN/N leu1-*

	32
FY10411	*h⁻ chp1::KanMX6 GBD-clr4-Δcd-HphMX6 ura4::3gbs-ade6⁺ ade6-DN/N leu1-32*
FY10416	*h⁻ rik1::KanMX6 GBD-clr4-Δcd-HphMX6 ura4::3gbs-ade6⁺ leu1-32*
FY10473	*h⁺ GBD-clr4⁺-HphMX6 ade6-210 otrISphI:ade6⁺ ura4-D18*
FY10515	*h? GBD-clr4-Δcd ade6-704 cc2:his3 ura4-D18 leu1-32 his3-D1*
FY10521	*h⁺ GBD-clr4-Δcd-NatMX6 ura4::3gbs-ade6⁺ arg3-D4 his3-D1 H3.1::his3⁺ H3.3::arg3⁺ .*
FY10524	*h⁻ GBD-clr4-Δcd-NatMX6 ura4::3gbs-ade6⁺ arg3-D4 his3-D1 H3.1::his3⁺ H3.3::arg3⁺ H3.2K9R-HphMX6*
FY10525	*h⁺ GBD-clr4-Δcd-NatMX6 ura4::3gbs-ade6⁺ arg3D his3D H3.1::his⁺ H3.3::arg⁺ H3.2K9A-HphMX6*
FY10594	*h⁺ GBD-clr4-Δcd-HphMX6 ura4::10gbs-ura4⁺ ade6-DN/N*
FY10676	*h⁻ ade6- ura4::3gbs-ade6⁺ GBD-clr4-Δcd-H410K-NatMX6*
FY10815	*h⁺ ura4::10gbs-ura4⁺ leu1-32*
FY10817	*h⁻ GBD-clr4-Δcd-HphMX6 ura4::10gbs-ura4⁺ leu1-32*
FY11240	*h⁻ clr3::KanMX6 GBD-clr4-Δcd-HphMX6 ura4::3gbs-ade6⁺ leu1-32*
FY11250	*h⁻ ura4::3gbs-ade6⁺ GBD-clr4-Δcd-HphMX6 swi6::NatMX6*
FY11252	*h⁻ ura4::3gbs-ade6⁺ GBD-clr4-Δcd-HphMX6 sir2::NatMX6*
FY11254	*h⁻ ura4::3gbs-ade6⁺ GBD-clr4-Δcd-HphMX6 chp2::KanMX6*
FY11338	*h⁻ dcr1::NatMX6 GBD-clr4-Δcd-HphMX6 ade6-DN/N*
FY11340	*h⁻ dcr1::NatMX6 GBD-clr4-Δcd-HphMX6 ura4::3gbs-ade6⁺ ade6-DN/N*
FY11897	*h⁹⁰ dcr1::NatMX6 GBD-clr4-Δcd-HphMX6 ade6-210*
FY11898	*h⁻ dcr1::NatMX6 GBD-clr4-Δcd-HphMX6 ade6-210*
FY11901	*h⁺ dcr1::NatMX6 ura4::3gbs-ade6⁺ ade6-DN/N*
FY11902	*h⁺ rik1::KanMX6 ura4::3gbs-ade6⁺ ade6-210*
FY11907	*h⁻ rik1::KanMX6 GBD-clr4-Δcd-HphMX6 ade6-DN/N*
FY11908	*h? GBD-clr4-Δcd-HphMX6 dcr1::NatMX6 ade6-704 cc2:his3 ura4-D18 leu1-32 arg3-D4?*
FY12048	*h⁻ dcr1::NatMX6 ura4::3gbs-ade6⁺ GBD-clr4-Δcd-HphMX6 ade6-DN/N*
FY12049	*h⁻ rik1::KanMX6 ura4::3gbs-ade6⁺ GBD-clr4-Δcd-HphMX6 ade6-DN/N*
FY12111	*h⁻ GBD-clr4⁺-HphMX6 ura4::3gbs-ade6⁺ ade6-DN/N*
FY12112	*h⁻ GBD-clr4-Δcd-H410K-HphMX6 ura4::3gbs-ade6⁺ ade6-DN/N*
FY12144	*h- 3xFlag-ago1-KanMX6 GBD-clr4-Δcd-H410K-HphMX6 ura4::10gbs-ura4⁺ ade6-DN/N*
FY12146	*h⁺ arg3::3gbs-ade6⁺ his3-D1 leu1-32 ura4-D18 ade6-210*

FY12147	*h^{+} GBD-clr4-Δcd-HphMX6 arg3::3gbs-ade6^{+} ade6-DN/N*
FY12148	*h^{-} GBD-clr4-Δcd-HphMX6 arg3::3gbs-ade6^{+} ade6-DN/N*
FY12149	*h^{+} GBD-clr4-Δcd-H410K-HphMX6 arg3::3gbs-ade6^{+} ade6-210*
FY12150	*h^{-} GBD-clr4-Δcd-H410K-HphMX6 arg3::3gbs-ade6^{+} ade6-DN/N*
FY12151	*h^{+} GBD-clr4-Δcd-HphMX6 arg3::3gbs-ade6^{+} ade6-DN/N*
FY12236	*h^{-} ade6-210 arg3-D4 his3-D1 ura4-D18 ars1::pREP3x-ura4-HP-LEU2*
FY12272	*h$^{?}$ 3xFlag-ago1-KanMX6 ura4::10gbs-ura4^{+}*
FY12343	*h? rik1::KanMX6 GBD-clr4-Δcd-HphMX6 ade6-704-NatMX6 ura4-DSE leu1-32 cc2:his3 his3-D1*
FY12471	*h- 3xFlag-ago1-KanMX6 GBD-clr4-Δcd-HphMX6 ura4::3gbs-ade6+ ade6-210*
FY12472	*h- 3xFlag-ago1-KanMX6 clr4 ura4::3gbs-ade6^{+} ade6-DNN*
FY12803	*h^{+} GBD-clr4^{+}-HphMX6 ura4::10gbs-ura4^{+} ade6-DN/N*
FY12769	*h^{-} dcr1::NatMX6 ura4::3gbs-ade6^{+} ade6-DN/N*
FY12780	*h^{-} rik1::KanMX6 ura4::3gbs-ade6^{+} ade6-DN/N*
FY12959	*h^{+} arg3::3gbs-ade6 his3-D1 leu1-32 ura4-D18 ade6-DNN*
FY13406	*h^{-} GBD-clr4-Δcd-HphMX6 ura4::3gbs-ade6^{+} ade6-DN/N his3-D1*
FY13408	*h^{-} GBD-clr4-Δcd-HphMX6 ura4::3gbs-ade6^{+} ade6-DN/N his3-D1*
FY13412	*h^{+} GBD-clr4-Δcd-HphMX6 ura4::3gbs-ade6^{+} ade6-DN/N his3-D1*
FY13552	*h^{-} rik1::KanMX6 ura4::3gbs-ade6^{+} ade6-DN/N his3-D1 leu1-32*
FY13554	*h^{-} rdp1::natMX6 GBD-clr4-Δcd-HphMX6 ade6-DN/N his3-D1*
FY13556	*h^{-} tas3::KanMX6 GBD-clr4-Δcd-HphMX6 ade6-DN/N*
FY13557	*h^{-} ago1::KanMX6 GBD-clr4-Δcd-HphMX6 ade6-DN/N*
FY13710	*h^{+} GBD-clr4-Δcd-NatMX6 ura4::3gbs-ade6^{+} ade6-DN/N*
FY13711	*h^{-} GBD-clr4-Δcd-NatMX6 ura4::3gbs-ade6^{+} ade6-DN/N*
FY13712	*h^{-} ura4::3gbs-ade6^{+} ade6-DN/N*
FY13714	*h^{-} dcr1::NatMX6 GBD-clr4-Δcd-NatMX6 ura4::3gbs-ade6^{+} ade6-DN/N*
FY13715	*h^{-} dcr1::NatMX6 GBD-clr4-Δcd-NatMX6 ura4::3gbs-ade6^{+} ade6-DN/N*
FY13716	*h^{90} dcr1::NatMX6 GBD-clr4-Δcd-NatMX6 ura4::3gbs-ade6^{+} ade6-DN/N*
FY13717	*h^{90} dcr1::NatMX6 GBD-clr4-Δcd-NatMX6 ura4::3gbs-ade6^{+} ade6-DN/N*
FY13917	*h^{90} clr3::KanMX6 GBD-clr4-Δcd-HphMX6 ade6-DN/N*

Table S2. List of oligonucleotides used in this study

Primer	Sequence	Experiment
DF121	AGGCGATTAAGTTGGGTAAC	ChIP (*0/3xgbs* region A)
DF191	GGTATCAGCTCACTCAAAGG	ChIP (*3xgbs* region F)
DF186	AAGGCGAGTTACATGATCC	ChIP (*3xgbs* region G)
DF187	AACGCTGGTGAAAGTAAAAG	ChIP (*3xgbs* region G)
DF192	GGTTGGACTCAAGACGATAG	ChIP (*3xgbs* region F)
DF217	TTTTCTGGCCTATTAGAACG	ChIP (*0xgbs* region B_0)
DF218	CAGAAACCTGAAGAGGAAAG	ChIP (*0xgbs* region B_0)
DF219	ATTAACCTAAGATGCAGGTG	ChIP (0/3xgbs region A)
DF220	CTTCCTTTTTGGTGTGTTTC	ChIP (0/3xgbs region C)
DF221	ACGTTGTTCACTGAAACCTC	ChIP (0/3xgbs region C, E)
DF238	GTGGTGAGGTAAACGAAATC	ChIP (3*xgbs* region B)
DF239	CCTGTTTTTCGCTCATATTC	ChIP (3*xgbs* region B)
qURA_FOR	AATACCGTCAAGCTACAATATGCATCTGGTG	qRT-PCR
qURA_REV	GGTTTTCTCTGTGTAGGAACCAGTAGCC	qRT-PCR
qACT_FOR	GGTTTCGCTGGAGATGATG	qRT-PCR
qACT_REV	ATACCACGCTTGCTTTGAG	qRT-PCR
WA26	AACAATAAACACGAATGCCTC	ChIP (*cc1/3*)
WA27	ATAGTACCATGCGATTGTCTG	ChIP (*cc1/3*)
WA28	CACATCATCGTCGTACTACAT	ChIP (*otr*)
WA29	GATATCATCTATATTTAATGACTACT	ChIP (*otr*)
WA33	AATGACAATTCCCCACTAGCC	ChIP (*fbp1*)
WA34	ACTTCAGCTAGGATTCACCTGG	ChIP (*fbp1*)
WA293	CAACTTTACTAATTTGACTCC	ChIP (*cc2,* region D)
WA295	CCAACTGATCCTTCAAACTAC	ChIP (*cc2,* region D)
act_mb86	AACCCTCAGCTTTGGGTCTT	qRT-PCR qChIP (*act1*)
act_mb87	TTTGCATACGATCGGCAATA	qRT-PCR qChIP (*act1*)
qAde6_NN_rev	TGAATTGAGAAGGGAAGACGAG	qRT-PCR qChIP (*ade6*)
qAde6_NN_fwd	ATGCTTATCCTACAACTGAGACC	qRT-PCR qChIP (*ade6*)
qDgI_rev	GGGTTCATCGTTTCCATTCAG	qPCRChIP (*otr)*

qDgI_fwd	AATTGTGGTGGTGTGGTAATAC	qChIP (*otr*)
qUra4_5'_fwd	TCGCAGACATTGGAAATACC	qChIP (*3xgbs*)
qUra4_5'_rev	ATGGCAATTTGTGATATGAGC	qChIP (*3xgbs*)
qUra4_SE_fwd	CGTGGTCTCTTGCTTTTGG	qRT-PCR (*ura4*)
qUra4_SE_rev	GTAGTCGCTTTGAAGGTTAGG	qRT-PCR (*ura4*)
ura4_L1_fwd	TCAGCATATCTTTCCACACTTG	qChIP (*ura4* -1 Kb)
ura4_L1_rev	TGAGAGGGAGTTTGAACCG	qChIP (*ura4* -1 Kb)
ura4_R1_rev	ACTCAGCATTCTTTCTCTAAATAGG	qChIP (*ura4* +1 Kb, *0/3xgbs* region E)
ura4_R1_fwd	ACAAACAAATACACTAGGTAAATCG	qChIP (*ura4* +1 Kb)
ura4_L2_fwd	CAGTTAGTTTCAGGTTTCCC	qChIP (*ura4* -2 Kb)
ura4_L2_rev	GCAGAGTAATGGTGATTGG	qChIP (*ura4* -1 Kb)
ura4_R2_fwd	TCATTACGGTCTGGCATCAAC	qChIP (*ura4* +2 Kb)
ura4_R2_rev	TCATCCTCCATTTCTCAAAGTCC	qChIP (*ura4* +2 Kb)
ura4_L3_fwd	ATCTCCTTCCCTCCTTTAACG	qChIP (*ura4* -3 Kb)
ura4_L3_rev	ATGCTGACGCTCTGTGTAC	qChIP (*ura4* -3 Kb)
ura4_R3_fwd	CCTTGGTAAACTCTCCGTTC	qChIP (*ura4* +3 Kb)
ura4_R3_rev	GGCTTGGAAGAAGTCTTTCG	qChIP (*ura4* +3 Kb)
ura4_L4_rev	CGTATGGACATGAGGCTCTC	qChIP (*ura4* -4 Kb)
ura4_L4_fwd	TAGGAAACTCCGTATCCCTTTAG	qChIP (*ura4* -4 Kb)
ura4_R4_fwd	CCGCTTCTACCATCTGACTG	qChIP (*ura4* +4 Kb)
ura4_R4_rev	ACTCTTAGGAAACCCAAATTCATC	qChIP (*ura4* +4 Kb)
ura4_L5_fwd	TTATCAAGCGTTGTTCATATAATTG	qChIP (*ura4* -5 Kb)
ura4_L5_rev	AGTGTCGCACCATCTAAGG	qChIP (*ura4* -5 Kb)
ura4_R5_fwd	TATACAACTGCTGCTAATCCTAG	qChIP (*ura4* +5 Kb)
ura4_R5_rev	CGCCTCTAATTTCCCTTTCG	qChIP (*ura4* +5 Kb)
ura4_R7_fwd	TGCCATTGCTCTTTTCATTGC	qChIP (*ura4* +7 Kb)
ura4_R7_rev	GTTCACCTCCGCCTCCAG	qChIP (*ura4* +7 Kb)
ura4_L10_fwd	ACCAGTAGTGAAACGACGAAATC	qChIP (*ura4* -10 Kb)
ura4_L10_rev	GCCCGTATGCTCCCTTGC	qChIP (*ura4* -10 Kb)
ura4_R10_rev	TCGTTCAACTCAACCGTAGG	qChIP (*ura4* +10 Kb)
ura4_R10_fwd	ATGCCCATTAAATCTCTTCACTG	qChIP (*ura4* +10 Kb)
IK8	ATTCCTTTCTGAACCTCTCTGTTAT	siRNA detection
IK9	TTTGATGCCCATGTTCATTCCACTTG	siRNA detection
IK10	GGGAGTACATCATTCCTACTTCGATA	siRNA detection

snR58	GATGAAATTCAGAAGTCTAGCATC	siRNA detection
ade6_FW	ATGAGCGAAAAACAGGTTGTAGGG	siRNA detection
ade6_RV	CTATGCAGAATAATTTTTCCAACC	siRNA detection

References

1. B. S. Wheeler, J. A. Blau, H. F. Willard, K. C. Scott, *PLoS Gen*. **5**, 4 (2009).
2. H. D. Folco, A. L. Pidoux, T. Urano, R. C. Allshire, *Science* **319**, 94 (2008).
3. R. C. Allshire, E. R. Nimmo, K. Ekwall, J. P. Javerzat, G. Cranston, *Genes Dev.* **9**, 218 (1995).
4. S. Moreno, A. Klar, P. Nurse, *Methods in Enzymology* **194**, 795 (1991).
5. P. Hentges, B. Van Driessche, L. Tafforeau, J. Vandenhaute, A. M. Carr, *Yeast* **22**, 1013 (2005).
6. M. Baum, V. K. Ngan, L. Clarke, *Mol. Biol. Cell* **5**, 747 (1994).
7. A. Pidoux, B. Mellone, R. Allshire, *Methods* **33**, 252 (2004).
8. T. Nakagawachi *et al.*, *Oncogene* **22**, 8835 (2003).
9. K. Ekwall *et al.*, *Science* **269**, 1429 (1995).
10. B. Kniola *et al.*, *Mol. Biol. Cell* **12**, 2767 (2001).
11. M. W. Pfaffl, *Nucleic Acids Res*. **29**, e45 (2001).